



**HAL**  
open science

## Fracture mechanics concepts applied to PVDF polymeric material exhibiting porosity, time and temperature dependency

Lucien Laiarinandrasana, Mélanie Lafarge, Gilles Hochstetter

### ► To cite this version:

Lucien Laiarinandrasana, Mélanie Lafarge, Gilles Hochstetter. Fracture mechanics concepts applied to PVDF polymeric material exhibiting porosity, time and temperature dependency. ECF 17, Sep 2008, Brno, Czech Republic. pp.1562-1569. hal-00329769

**HAL Id: hal-00329769**

**<https://hal.science/hal-00329769>**

Submitted on 5 Jun 2013

**HAL** is a multi-disciplinary open access archive for the deposit and dissemination of scientific research documents, whether they are published or not. The documents may come from teaching and research institutions in France or abroad, or from public or private research centers.

L'archive ouverte pluridisciplinaire **HAL**, est destinée au dépôt et à la diffusion de documents scientifiques de niveau recherche, publiés ou non, émanant des établissements d'enseignement et de recherche français ou étrangers, des laboratoires publics ou privés.

## Fracture mechanics concepts applied to PVDF polymeric material exhibiting porosity, time and temperature dependency

L. Laiarinandrasana<sup>1, a</sup>, M. Lafarge<sup>1, 2, b</sup> and G. Hochstetter<sup>3, c</sup>

<sup>1</sup>Centre des Matériaux–Mines ParisTech – CNRS UMR 7633 BP 87 F-91003 Evry Cedex - France

<sup>2</sup>ARKEMA, CRRA – Rue Henri Moissan BP 63, F-69493 Pierre Bénite Cedex - France

<sup>3</sup>ARKEMA – CERDATO, F-27470 Serquigny - France

<sup>a</sup>lucien.laiarinandrasana@ensmp.fr, <sup>b</sup>melanie.lafarge@arkemagroup.com, <sup>c</sup>gilles.hochstetter@arkemagroup.com

**Keywords:** Polymer, Fracture Mechanics, Local approach, Finite Elements, Porous media.

**Abstract.** The Polyvinylidene fluoride (PVDF) under study is a semi-crystalline polymer that exhibits significant initial porosity and sensitivity on mechanical properties to both strain rate and temperature. A comprehensive experimental database was built in order to analyze the fracture behavior in the ductile to brittle transition domain.

Experimental data on smooth and notched specimens were produced at temperature ranging from -50°C to 20°C. They were used to determine temperature dependent material parameters by using the mechanics of porous media. The obtained set of parameters was validated on two kinds of pre-cracked specimens, by using the local approach of fracture mechanics. With the help of a finite element code, both global and local approaches of fracture mechanics were shown to complement one another: whereas classical formulae of J-integral fail to characterize crack initiation for this PVDF, the present methodology allowed the plot of  $J_{IC}$  values with respect to temperature.

### Introduction

Fracture mechanics concepts are useful tools for assessing engineering components. The global approach taking benefit of load parameters such as stress intensity factor, energy release rate or J-integral has been used for years, especially for metallic materials. Applying these concepts for polymeric materials is not straightforward and much care has to be taken.

The laboratory Polyvinylidene fluoride (PVDF) under study is a semi-crystalline polymer with an initial porosity of about 10%. Moreover, experimental results evidenced that this PVDF can be considered as a temperature dependent viscous material.

An attempt was made to use J-integral concept on pre-cracked specimens with analytical formulation [1]. This approach requires elastic-plastic material coefficients such as Ramberg-Osgood hardening parameters, so that neither the viscous deformation nor the porosity of the material can be taken into account.

The local approach of fracture mechanics seems to be an alternative method to overcome this difficulty, insofar as it is supposed to integrate the deformation and damage mechanisms in the process zone (next to the crack tip). The use of finite element (FE) method is needed. The implementation of constitutive relations able to reproduce any aspect of the deformation and damage mechanisms within the FE code is a pre requisite.

In this study, both global and local approaches of fracture mechanics were addressed with the help of an in-house FE code [2]. Both approaches are shown to complement one another. First, experimental data obtained for the PVDF under study at various temperatures were used to identify material coefficients dealing with the mechanics of porous media. FE computations of cracked specimens at selected temperatures were then performed in order to check the ability of the model to

simulate crack initiation and growth. In order to complete the experimental database at every investigated temperature and with two kinds of cracked specimen geometries, some numerical results taking advantage of the local approach of fracture mechanics were produced. This database was then utilized to come back to the global approach of fracture mechanics. The aim was to compute J-integral evolution of each test by means of FE analysis. This gives access to  $J_{IC}$  and allows the plot of  $J_{IC}$  against the test temperature.

### Experimental procedures

The material of interest is a specific grade of Polyvinylidene Fluoride (PVDF), produced by Arkema. Since the study did not focus on aging effects, the material was extruded without plasticizer. This resulted in a significant void volume ratio. The initial amount of porosity was estimated to 10% [3]. To obtain this value, some samples of the material were broken in liquid nitrogen. The fracture surfaces were then examined with the help of a scanning electron microscope (SEM). The porosity was calculated as the area fraction of cavities. The glass transition temperature is  $T_g \approx -40^\circ\text{C}$ .

The experimental database consists of tests on smooth tensile specimens, on cylindrical notched tensile (CNT) specimens with four values of the notch radii (4mm, 1.6mm and 0.8mm), of precracked double edge notched tensile (DENT) specimens and of precracked single edge notch bending (SENB) specimens.

Smooth and CNT tests results at  $20^\circ\text{C}$  were published elsewhere [3]. The database at various temperatures ranging from  $-50^\circ\text{C}$  to  $20^\circ\text{C}$  is available in [4]. A paper devoted to the modeling of these latter tests is under preparation. Besides the large amount of initial porosity, the PVDF under study exhibits strain rate sensitivity and temperature dependency.

In this paper, attention is paid to pre-cracked specimens. The characteristic dimensions of DENT specimens are as follows: width  $W = 6\text{mm}$ , thickness  $B = 12\text{mm}$  and a gauge length of about 110mm. SENB specimens are 14mm wide, 7mm thick and 76mm long. The precracks (noted  $a$ ) are implanted onto the specimens by using a fresh razor blade. Selected tests are displayed in Table 1 and Table 2. Fig.1 illustrates the load versus opening displacement for the selected tests. Strain rate dependency was investigated at room temperature ( $20^\circ\text{C}$ ). The other temperatures were alternatively selected for each specimen geometry in such a way that every  $10^\circ\text{C}$  one test is performed on a pre-cracked body.

Test reference	Temperature	a/W
DENT12	$20^\circ\text{C}$	0.46
DENT9	$0^\circ\text{C}$	0.47
DENT25	$-20^\circ\text{C}$	0.46
SENB2	$20^\circ\text{C}$	0.49
SENB9	$-10^\circ\text{C}$	0.48
SENB10	$-30^\circ\text{C}$	0.49

Table 1: Selected tests on DENT and SENB specimens at various temperatures and for a crosshead speed of about 0.15mm/s

The crack propagation was monitored using a video camera, except for very low temperature where the nitrogen gas used for thermal regulation alters the image resolution. At the end of each test, fracture surfaces examinations were carried out. Two kinds of fracture surface patterns were observed. The first one will be called "ductile surface". It looks whitened and rather "flat".

Elongated fibrils clearly appear, supposed to result from crazed microstructure. The second one is called “brittle surface”. There is no apparent deformation of the microstructure. Typically, brittle surface looks like fracture surfaces obtained at the liquid nitrogen temperature.

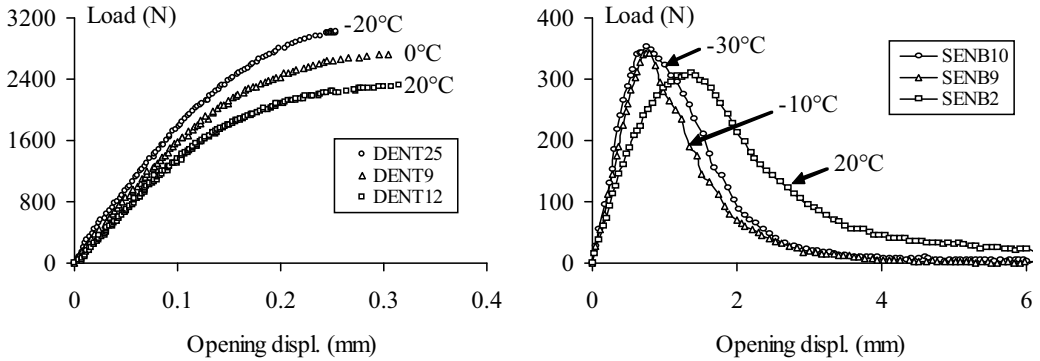


Figure 1: Load versus opening displacement curves of PVDF at various temperatures

With these definitions, it turns out that the fracture surface of SENB specimens is totally ductile even at the lowest temperature of -30°C. Video acquisition indicates that the crack propagates in a stable manner. The crack growth rate is moderate. The fracture surfaces of DENT specimens exhibited an initial part looking like “ductile” followed by a transient region and then by “brittle” pattern. The crack starts to propagate in a stable way, then accelerates until reaching a critical crack growth rate and finishes in brittle manner with a very high speed.

### Modelling

The PVDF of interest exhibits significant initial void volume fraction ( $f_0 = 0.1$ ). An attempt was made to take it into account in constitutive equations by using the mechanics of porous media. The Gurson-Tvergaard-Needleman (GTN) [5,6,7] yield function (Eq. 1) was modified in order to take strain rate sensitivity, as well as rheo-hardening into account.

$$\Phi(\sigma, \sigma^*, f) = \frac{\sigma_{eq}^2}{\sigma^{*2}} + 2q_1 f \cosh\left(\frac{q_2 \sigma_{kk}}{2\sigma^*}\right) - 1 - q_1^2 f^2 = 0 \quad (1)$$

$\sigma_{eq}$  is the von Mises stress, and  $\sigma_{kk}$  is the trace of the stress tensor.  $f$  is the porosity,  $f_0$  is the initial value of the void volume fraction,  $q_1$  and  $q_2$  are model damage parameters. The yield surface reads:

$$\varphi = \sigma^* - R \quad (2)$$

where  $R$  is the flow stress of the matrix material:

$$R = R_0 + Q(1 - e^{-bp}) + A(e^{Bp} - 1) \quad (3)$$

where  $R_0$ ,  $Q$ ,  $b$ ,  $A$ ,  $B$  are material parameters and  $p$  is the cumulative plastic strain. The second term  $Q(1 - e^{-bp})$  describes the initial hardening stage, whereas the latter  $A(e^{Bp} - 1)$  allows the

simulation of the large stretching of the fibrils, which leads to a rapidly increasing stress (reohardening).

The normality rule yields the expression of the viscoplastic strain rate tensor:

$$\dot{\underline{\epsilon}}_{vp} = (1 - f) \dot{p} \frac{\partial \Phi}{\partial \underline{\sigma}} \quad (4)$$

$\dot{p}$  is obtained by using the matrix viscoplastic Norton law:

$$\dot{p} = \left\langle \frac{\Phi}{K} \right\rangle^n \quad (5)$$

$K$ ,  $n$  are material parameters to be identified.

The evolution of porosity follows the equation of mass balance:

$$\dot{f} = (1 - f) \text{trace}(\dot{\underline{\epsilon}}_{vp}) \quad (6)$$

The void growth decreases when cavities become elongated [8]. This is accounted for by expressing  $q_2$  as a decreasing function of the maximum principal plastic strain  $p_1$ :

$$q_2 = \begin{cases} q_2^0 & \text{if } p_1 < p_1^t \\ 1 + e^{-3p_1} & \text{otherwise} \end{cases} \quad (7)$$

A number of material parameters were identified at 20°C [3,4]. In particular,  $v = 0.38$ ;  $b = 75$ ;  $A = 11 \text{ MPa}$ ;  $B = 1.6$  and  $q_1 = 0.8$  do not depend on temperature, whereas the remainder values are displayed in Table 2 with respect to the test temperature [4].

	20°C	0°C	-10°C	-20°C	-30°C	-50°C
E [MPa]	2000	2400	2600	2800	3000	3500
R <sub>0</sub> [MPa]	10	15	20	22	25	30
Q [MPa]	40	44	48	50	52	82
K [MPa]	20	20	25	25	30	40
n	5	6	7	7	7	7
q <sub>2</sub> <sup>0</sup>	1.55	1.60	1.65	1.65	1.70	1.82
p <sub>1</sub> <sup>t</sup>	0.2	0.15	0.15	0.15	0.15	0.15

Table 3: Optimised material parameters at various temperatures

The present set of parameters for the modified GTN model allows successful simulation of the global stress-strain curves for smooth and CNT specimens at various strain rates and temperatures.

Furthermore, a local criterion allowing prediction of crack initiation and growth under ductile tearing (stable cracking) was identified. A critical porosity  $f_c$  whose value is about 0.63 was identified together with a critical plastic strain value  $p_c$  for lower stress triaxiality ratios. Since only cracked specimens are concerned here (high stress triaxiality ratio), interest is focused on  $f_c$ .

These material parameters were first validated with the help of cracked specimen data at various temperatures (Table 1). To do this, FE computations were run under finite strain formulation on fully 3D meshes of both geometries.

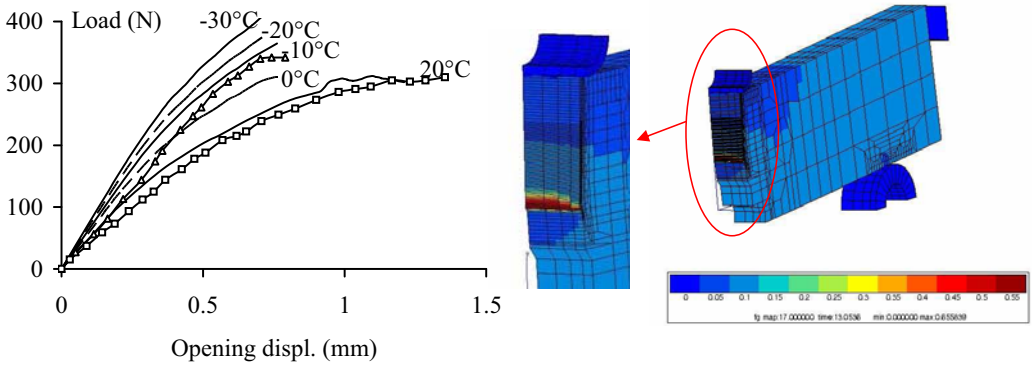


Figure 2: Simulation of SENB tests at various temperatures

Figs.2-3 summarize a typical comparison of the experimental database provided in Table 1 with the corresponding numerical simulations for respectively SENB and DENT specimens. The deformed meshes are presented in the right of each figure, whereas the plot (left hand) represents the load versus opening displacement.

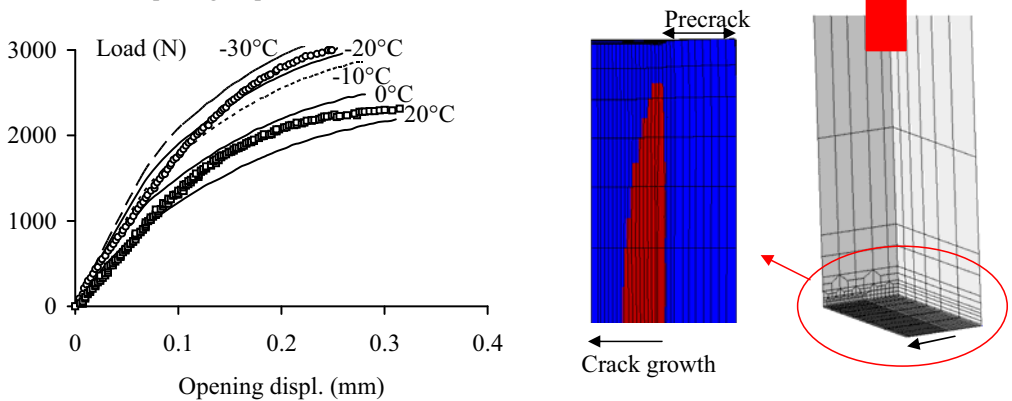


Figure 3: Simulation of DENT tests various temperatures

The contour maps of the porosity indicate that the present modeling was able to reproduce crack initiation and growth only by using the critical porosity  $f_c$ . One can access interesting variables next to the crack tip. For instance, focus on the deformed meshes in the vicinity of the crack tip clearly shows the numerical crack advance with its tunneling effect (curved crack front), the porosity distribution and the thickness reduction due to plane stress conditions at the side surface of the specimen. In this paper, attention is paid to the crack initiation only. The first broken elements at the crack tip (mid section) occur at the peak load. In the sequel, parameters corresponding to the crack initiation will be computed at this stage (peak load).

Fig.2 illustrates the load versus opening displacement for SENB test at various temperatures and prior to the crack initiation (stopped at the peak load). Comparisons between experimental and simulated curves are done at 20°C (open square symbols and corresponding solid line) and -10°C (open triangle symbols and corresponding solid line). At 20°C the numerical curve overestimates the experimental load whereas at -10°C this order is inverted. The experimental curve at -30°C was not plotted for the sake of clarity of the figure. Since the aforementioned comparisons were satisfactory, predicted simulated curves are plotted at 0°C and -20°C. Note that at these temperatures, material coefficients were validated with DENT specimens. Both curves interrupted at peak load were merged in Fig.2.

For DENT specimens the same comments as above corresponding to SENB specimens can be made. Good agreement was obtained by comparing experimental with simulated curves at 20°C (open square and corresponding solid line) and -20°C (open circles and corresponding solid line). At -10°C and -30°C material coefficients were validated with SENB tests. Therefore DENT tests at these temperatures were computed. With Figs.2-3, temperatures ranging from 20°C to -30°C are mapped (every 10°C) by using experimental and numerical results together.

The present model can then integrate the porosity, strain rate and temperature effects via the constitutive equations. The initiation and growth mechanisms of ductile tearing, emanating from pre-existing crack can be discussed in the light of this so-called local approach of fracture. The critical porosity  $f_c$  seems not to depend on temperature, at least from 20°C to -30°C. Load versus opening displacement curves were plotted. They are key figures for fracture mechanics concept, since the load parameter (J-integral) is essentially based on the area under this kind of curve.

### Fracture mechanics global approach

The main goal here consists of plotting the toughness  $J_{1C}$  values against the temperature, at least for ductile tearing initiation.  $J_{1C}$  is defined as the value of the J-integral at the peak load corresponding to first broken element. To this end, the aforementioned experimental and numerical results will be utilized. The J-integral determination was carried out with the FE code [2] by applying the De Lorenzi [9] approach. The FE computation is done with 2D with small deformation plane strain elements.

For DENT specimens, taken as an example, Fig.4a shows the evolution of the J-integral value during the loading stage at various temperatures. At crack initiation, J-integral drops down. The toughness  $J_{1C}$  value corresponds then to the maximum value of J-integral. Fig.4b plots all collected  $J_{1C}$  values for both specimens.

Fig.4b seems to indicate that  $J_{1C}$  value is about 63kJ/m<sup>2</sup> with a slight increase when the test temperature decreases. There is no effect of the specimen geometry on the value of  $J_{1C}$  [10]. The negative slope of the  $J_{1C}$  versus temperature curve is unexpected. The classical evolution of  $J_{1C}$  versus temperature is a S-type curve. Two asymptotic values of  $J_{1C}$  are considered: brittle (low value) and ductile (high value). The ductile to brittle transition temperature (DBTT) is theoretically determined from this curve. In the present study, the ductile value was obtained. The glass transition temperature of the PVDF under study is about -40°C. Unfortunately, no crack test was performed in the region of purely brittle fracture, probably at temperature lower than -40°C. Depending on these tests, a comparison can be made between  $T_g$  and the DBTT.

The negative slope of  $J_{1C}$  versus temperature may be due to the strain rate effect and the rheo-hardening incorporated into the constitutive equations. Further investigation has to be carried out to better understand this effect, namely concerning the self-heating of the specimen during the tests.

The same approach can be applied for crack growth under ductile tearing. In this case the resistance (J- $\Delta a$ ) curve slopes at various temperatures have to be compared.

All these comments about J-integral concept can alternatively be applied on other parameters of the global approach of fracture mechanics, such as the Essential Work of Fracture.

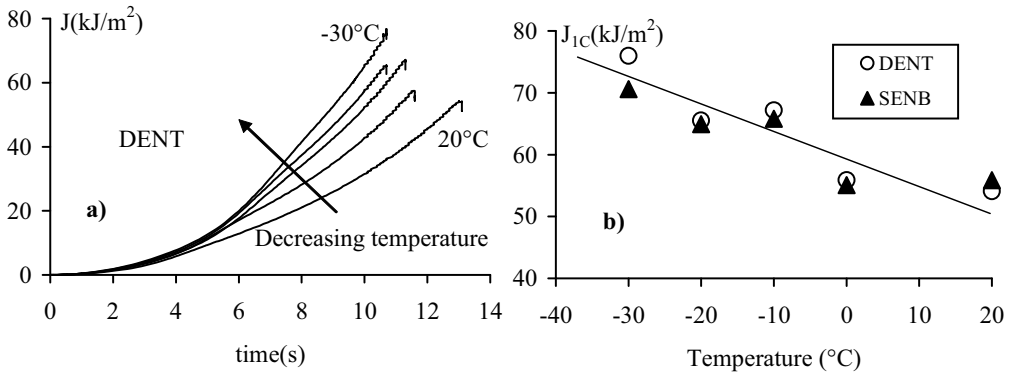


Figure 4 : J-integral and  $J_{1C}$  values at various temperatures

### Conclusion

The PVDF material under study exhibits significant initial porosity, temperature dependency and strain rate effects. Therefore, classical J-integral formula [1] fails to analyze crack initiation on DENT and SENB specimens.

Continuum mechanics of porous media framework was utilized in order to implement constitutive equations into a home made finite element code. The Gurson-Tvergaard-Needleman model was modified in order to take the porosity, the strain rate and temperature dependency into account. The set of material parameters was identified with tensile tests on smooth specimens and on round notched bars. Furthermore, by using the local approach of fracture mechanics it was shown that the crack initiation could be predicted when a critical porosity  $f_c$  is reached in the vicinity of the crack tip.

Taking advantage of the FE method that allows both local approach methodology and the J-integral computation, the evolution of toughness,  $J_{1C}$ , with respect to test temperature was plotted.  $J_{1C}$  was reported to have a mean value of about 63kJ/m<sup>2</sup> with a slight increase when the test temperature decreases. There is no effect of the specimen geometry on the value of  $J_{1C}$ . The negative slope of the  $J_{1C}$  versus temperature curve may be due to the strain rate effect and the rheo-hardening incorporated into the constitutive equations. Further investigation have to be carried out to better understand this effect, namely concerning self-heating of the specimen during the tests.

### References

- [1] V. Kumar, M.D. German, C.F. Shih: *An engineering approach for elastic-plastic fracture*, EPRI report NP 1931 (1981).
- [2] J. Besson, R. Foerch, *Computer Methods in Applied Mechanics and Engineering* Vol. 142 (1997), p. 165.
- [3] M. Challier, J. Besson, L. Laiarinandrasana, R. Piques: *Engineering Fracture Mechanics* Vol. 73 (2006) p. 79.
- [4] M. Lafarge, *Thesis, Ecole Nationale Supérieure des Mines de Paris*. (France 2004: in French).
- [5] A.L. Gurson: *J. Eng. Mater. Technol.* Vol. 99 (1977), p. 2.
- [6] V. Tvergaard: *J. Mech Phys Solids* Vol. 30 (1982), p. 399.
- [7] V. Tvergaard, A. Needleman: *Acta Metall.* Vol. 32 (1984), p. 157.



- [8] T. Pardoen and J.W. Hutchinson, *J. Mech. Phys. Solids*: Vol. 48(12) (2000), p. 2467.
- [9] H.G. De Lorenzi, *Engineering Fracture Mechanics*: Vol. 21(1) (1985), p. 129.
- [10] L. Laiarinandrasana, G. Hochstetter, M. Lafarge: *Proceedings of 16th European Conference of Fracture*, Alexandroupolis, Greece, July 3-7, 2006. Edited by E.E. Gdoutos. Cdrom 8pages